JOURNAL OF GEOPHYSICAL RESEARCH, VOL. 103, NO. A12, PAGES 29,383–29,391, DECEMBER 1, 1998

A self-consistent explanation for a plasma flow vortex associated with the brightening of an auroral arc

M. J. Kosch
Max-Planck-Institut für Aeronomie, Katlenburg-Lindau, Germany

M. W. J. Scourfield
Space Physics Research Institute, University of Natal, Durban, South Africa

E. Nielsen
Max-Planck-Institut für Aeronomie, Katlenburg-Lindau, Germany

Abstract. Simultaneous observations have been made of an auroral arc by an all-sky TV imager and of plasma flows near the arc by the Scandinavian Twin Auroral Radar Experiment. After the Harang Discontinuity, during a quiet geomagnetic interval ($Kp = 1^+$), the arc undergoes a sudden brightening during an eastward surge. This is accompanied by a vortex in the plasma drift velocities, poleward of the arc, of spatial extent 180 × 140 km. Westward drifts at higher latitudes merge with eastward drifts at lower latitudes near the arc. No radar backscatter was recorded equatorward of the arc. The plasma flow vortex is shown to correspond with an ionospheric region of diverging horizontal electric fields, which is equivalent to a downward field-aligned current. This region may correspond to black auroras. Spatial location of the closure current region associated with an arc by ground-based observations is a novel result.

1. Introduction

Baumjohann [1991] points out that it is reasonably straightforward to map the large-scale features of the electrojet systems, i.e., to determine the spatial and temporal variations of currents. This is experimentally undemanding because the convection currents vary slowly in time, longitude, and latitude. However, the precipitation of energetic particles in, for example, auroral arcs can result in small-scale longitudinal and latitudinal conductivity gradients. Such conductivity gradients, which can also be highly variable in time, occur within localized regions of as little as 1–20 km, the width of auroral arcs. The strong conductivity gradients modify the convection-driven electrojets and the associated convection electric fields. Measurements of electric fields, currents, and conductivities about a localized region of 20 km or less are rather difficult for satellite, rocket, and most ground-based experiments.

A concise summary of the various relationships that have been found to exist between electric fields and conductivities, in association with auroral arcs, is given by *Aikio et al.* [1993] and *Baumjohann* [1983]. *Marklund* [1984] points out that there are two ways to maintain current continuity across an arc, namely, by polarization electric fields and by Birkeland currents. *De la Beaujardiere et al.* [1981] and *Marklund* [1984] have suggested categories for arcs based on the (polarization) electric fields and Birkeland currents associated with arcs. There have been numerous observations [e.g., *Evans et al.*, 1977; *Horwitz et al.*, 1978; *Cahill et al.*, 1980; *Stiles et al.*, 1980; *de la Beaujardiere et al.*, 1981; *Marklund et al.*, 1982; *Ziesolleck et al.*, 1983; *Brüning and Goertz*, 1986; *Timofeev et al.*, 1987; *Opgenoorth et al.*, 1990; *Valladares and Carlson*, 1991; *Aikio et al.*, 1993; *Lewis et al.*, 1994] of enhanced electric field equatorward (poleward) of an arc in the premidnight (postmidnight) sector. In fact, this is a common feature of arcs at all local times [*Opgenoorth et al.*, 1990]. Electric field enhancements of up to 100 mV/m or more, generally much larger than the convection field, may occur [*Aikio et al.*, 1993; *Opgenoorth et al.*, 1990]. Such regions of electric fields have been referred to as a "radar arc" because coherent radar backscatter also occurs here. *Timofeev et al.* [1987] found that postmidnight radar arcs appear or suddenly intensify with the optical brightening of the associated auroral arc.

Aikio et al. [1993] have proposed the following scenario. Satellite measurements have shown that the current system associated with auroral arcs consists of a matched pair of Birkeland currents. The upward current flowing from the arc and the downward return current flowing on the poleward (equatorward) side of the arc in the postmidnight (premidnight) sector are connected by a Pedersen current in the ionosphere. Since the Pedersen current will flow in the direction of the convection electric field (equatorward postmidnight and poleward premidnight), this determines on which side of the optical arc the radar arc is observed. The upward current is carried by the energetic precipitating electrons responsible for the auroral arc. The downward current is carried by upward moving, cold ionospheric electrons outside of the arc, resulting in a depletion of ionospheric conductivity in that region. If the magnetospheric process resulting in an auroral arc acts as a current generator, the ionospheric electric field has to modify itself in such a way that current continuity in the ionosphere is preserved. Therefore the meridional electric field has to increase in order to produce an enhanced ionospheric Pedersen current to support the enhanced downward current in response to the increased upward current above the arc. *Tsunoda et al.*

Paper number 98JA02480.
0148-0227/98/98JA-02480$09.00

[1976] and *Timofeev et al.* [1987] have shown that the radar aurora corresponds to downward field-aligned currents linked to the visual aurora by an ionospheric Pedersen current.

Several authors [e.g., *Opgenoorth and Baumjohann*, 1984; *Opgenoorth et al.*, 1983a, b; *Aikio et al.*, 1993] have demonstrated, for specific case studies of active auroras (optically enhanced arcs, westward surges, and omega bands), that it is possible to reproduce the observed electric field by a superposition of an electric field due to the auroral form (directed perpendicularly to the form at all points along it) upon the background electric field.

Black aurora is the lack of optical emission in a small, well-defined region within an otherwise uniform, diffuse background [*Davis*, 1978]. The optical intensity within the black aurora is that of the background sky [*Schoute-Vanneck et al.*, 1990; *Trondsen and Cogger*, 1997]. The phenomenon generally appears as east-west aligned arc segments, filaments, or patches that drift eastward in the postmidnight sector [*Schoute-Vanneck et al.*, 1990; *Trondsen and Cogger*, 1997]. Black auroras have been observed only within 30° of the magnetic zenith [*Davis*, 1978], implying that the phenomenon has limited vertical extent. Black auroras appear to be a common feature of late recovery phase of an auroral substorm [*Trondsen and Cogger*, 1997]. However, very little information on the phenomenon is contained in the literature, with the first report probably by *Parsons and Thomas* [1973]. This is almost certainly due to the difficulting of recording such events, even though one of us (M. J. Kosch) has frequently observed them by eye from northern Scandinavia. *Trondsen and Cogger* [1997] measured 31 black auroral patches and arc segments and found a typical width of 0.5–1.5 km, length of 2.5–3 km, and drift speed of 0.6–1.5 m/s. *Schoute-Vanneck et al.* [1990] measured 40 black filaments to find a typical width of 1 km, length of 5–20 km, and drift speed of 1–3.9 km/s. Black auroras may exhibit shear, forming streets of vortices [*Davis*, 1978] with opposite rotation to the more familiar auroral curls [*Hallinan and Davis*, 1970], implying that they correspond to regions of positive space charge. Large, radially divergent electric fields (≈1 V/m), implying a positive space charge, have been observed by the Freja satellite on a small-scale size (≈1 km) at low altitudes (<1700 km), mostly in the postmidnight sector [*Marklund et al.*, 1994, 1995]. The measurements correspond to a complete lack of electron precipitation in regions of downward field-aligned current (2 $\mu A/m^2$), depleted thermal plasma (Pedersen conductance <1 S), and significant wave activity. *Marklund et al.* [1994, 1995] associated these measurements with the black aurora, although no direct optical observations were available. Theories involving wave phenomena have been advanced to explain black aurora [*Mishin and Förster*, 1995; *Shukla et al.*, 1995]; however, insufficient observational evidence exists to be conclusive.

The results reported here were obtained primarily by two high-resolution systems, a low-light-level TV camera for optical imaging and the Scandinavian Twin Auroral Radar Experiment (STARE) [*Greenwald et al.*, 1978] for ionospheric plasma flows and electric fields. It was arranged for the optical field of view to include the area observed by the radar (67.6°–72.6°N, 13.5°–26.0°E). STARE is sensitive to electrostatic waves in the auroral E layer at ~105 km altitude [*Fejer and Kelley*, 1980]. The mean Doppler shift of these waves is used to deduce good approximations of the speed and direction of the electron Hall drift. This method gives two-dimensional maps of the plasma flow and hence electric field over a section of the auroral oval at those locations where the ionospheric electric field exceeds a threshold of ~15 mV/m [*Cahill et al.*, 1978]. The measurements are made with good spatial resolution (20 × 20 km) over a large area (500 × 500 km) and are carried out on a continuous basis with a time resolution of 10 s. Thus STARE provides a "window," rotating with Earth, through which the auroral oval E region plasma flow and electric field pattern can be monitored. In many of the above mentioned studies, the STARE system played a key role in experimentally determining the ionospheric electric fields around the auroral forms.

2. Observations

The data examined here were obtained at 2135 UT on January 15, 1980, close to magnetic midnight (≈2130 UT). Geomagnetic conditions were quiet with $\Sigma Kp = 12^-$ on this day and $Kp = 1^+$ for the period 2100–2400 UT, unusually low values for the auroral activity observed. An arc was imaged in white light by an all-sky, low-light-level TV camera system operated from Skibotn (69.35°N, 20.36°E, $L = 6$), Norway. Simultaneously, STARE was observing the ionospheric plasma flows within the imager's field of view with 10 s temporal resolution and 20 × 20 km spatial resolution. Black auroras were reported from the same data set only 4 min later, from 2139 to 2158 UT [*Schoute-Vanneck et al.*, 1990].

GEOS 2 satellite magnetometer and particle data [*Korth et al.*, 1978] are shown in Figure 1 using 1 min averages. GEOS 2 was located on a geostationary orbit on the Kiruna meridian (20.42°E), very close to the Skibotn meridian. The time of the event under study is shown by the arrow. The absolute magnetometer traces are shown in VDH coordinates, where H is parallel to the magnetic dipole axis (north positive), D is perpendicular to the radius vector connecting the center of Earth to the satellite (east positive), and V completes the right-handed orthogonal coordinate system. The data show very quiet magnetic conditions. Total integrated particle fluxes for electrons (>22 keV) and ions (>27 keV) are shown for the quasi-field-aligned (pitch angle (PA) < 25°) and quasi-field-perpendicular (75° < PA < 105°) directions. The particle flux data (and other pitch angles not shown) show isotropic and very quiet particle fluxes. The magnetosphere was in a quiet and steady state at the time of the event (A. Korth, private communication, 1997).

At 2134 UT a surge of luminosity propagated eastward along the arc at ≈4 km/s, causing enhanced brightness and some distortion of the arc. It was during the enhanced brightening of the arc, which attained its maximum 1 min later, that the plasma vortex was observed by STARE. The all-sky auroral image recorded at 2135 UT is shown in Figure 2. The geographic directions from Skibotn are indicated with north and east at the bottom and right-hand side of the image, respectively. The circle represents the idealized horizon corresponding to the ±90° all-sky field of view. Superimposed is the grid of STARE plasma flow vectors with the direction pointing away from each white dot. Locations with no vectors correspond to no radar backscatter. The radar data projection is for 100 km altitude. The patch of luminosity near the southwest horizon is an artifact of artificial illumination.

Figure 2 exhibits the customary spatial distortion associated with all-sky lenses, which are linear in local zenith and azimuth angle. This is particularly severe near the periphery of the field of view. Removal of this effect, by digital image processing, greatly eases analysis. Figure 3 shows a mapping of Figure 2

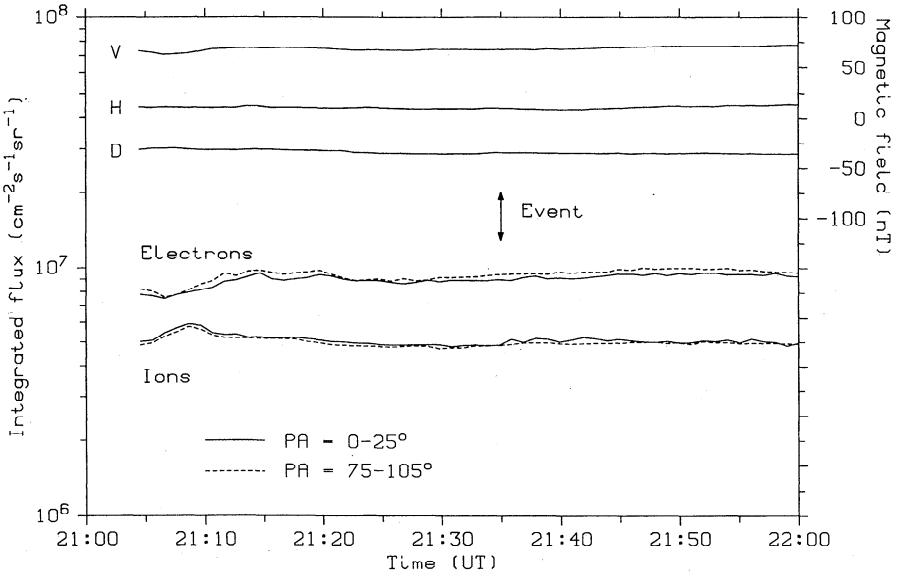

Figure 1. One hour of GEOS 2 geostationary satellite data, for the 20.42° geographic meridian, centered on the event. Absolute magnetometer traces are shown for the H, D, and V directions. The total integrated particle fluxes for electrons (>22 keV) and ions (>27 keV) are shown for the quasi-field-aligned (pitch angle (PA) < 25°) and quasi-field-perpendicular (75° < PA < 105°) directions.

onto a rectilinear geographic grid, for an altitude of 100 km, to remove the all-sky spatial distortion. The apparent radial streaking in the image near the edges is partially due to the vertical extent of the aurora. An anticlockwise plasma vortex is visible between 17° and 21° longitude and covers a region of ~180 × 140 km spatial extent. Westward drifts at higher latitudes merge with eastward drifts at lower latitudes near the arc. The plasma vortex drifted eastward at ~700–800 m/s and is associated with a moving distortion in the arc in the same range of longitudes.

Balsley et al. [1973] showed that a close relationship between the radar and visual aurora exists, with backscatter poleward of the luminosity postmidnight and vice versa. *Greenwald et al.* [1973] found the radar aurora to be mostly equatorward of the visual aurora in the evening sector; however, sometimes it was also reversed. Radar backscatter on both sides of arcs has been

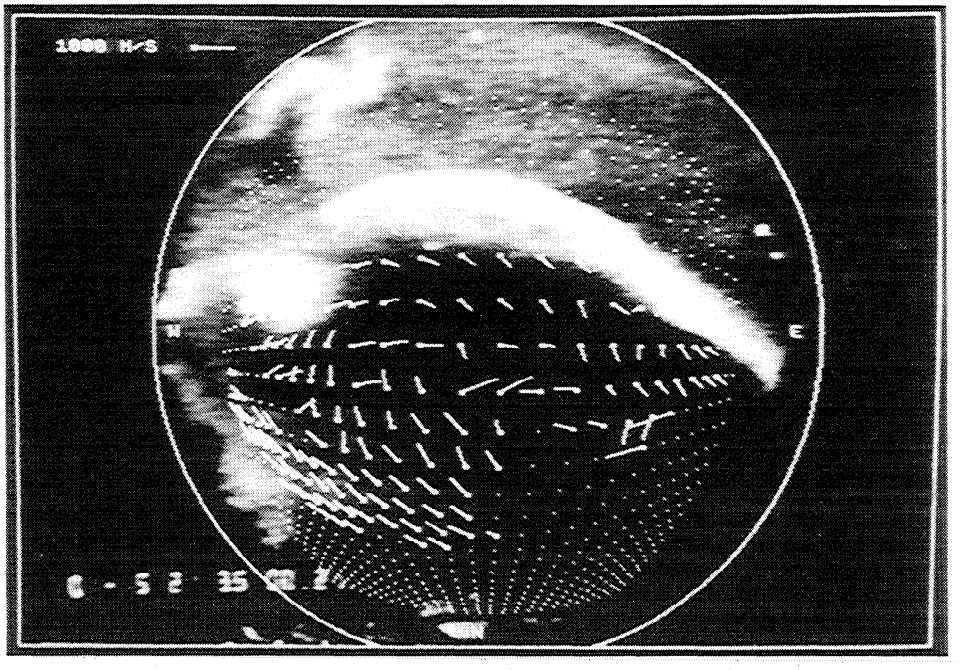

Figure 2. The all-sky, white-light TV image of the east-west aligned arc after it had brightened, taken at 2135 UT on January 15, 1980, from Skibotn (69.35°E, 20.36°N), Norway. The geographic directions are indicated. The circle represents the idealized ±90° all-sky field of view. Superimposed is a grid of Scandinavian Twin Auroral Radar Experiment (STARE) plasma flow vectors, with the direction pointing away from each white dot. Locations with no vectors correspond to no radar backscatter. The projection is for 100 km altitude.

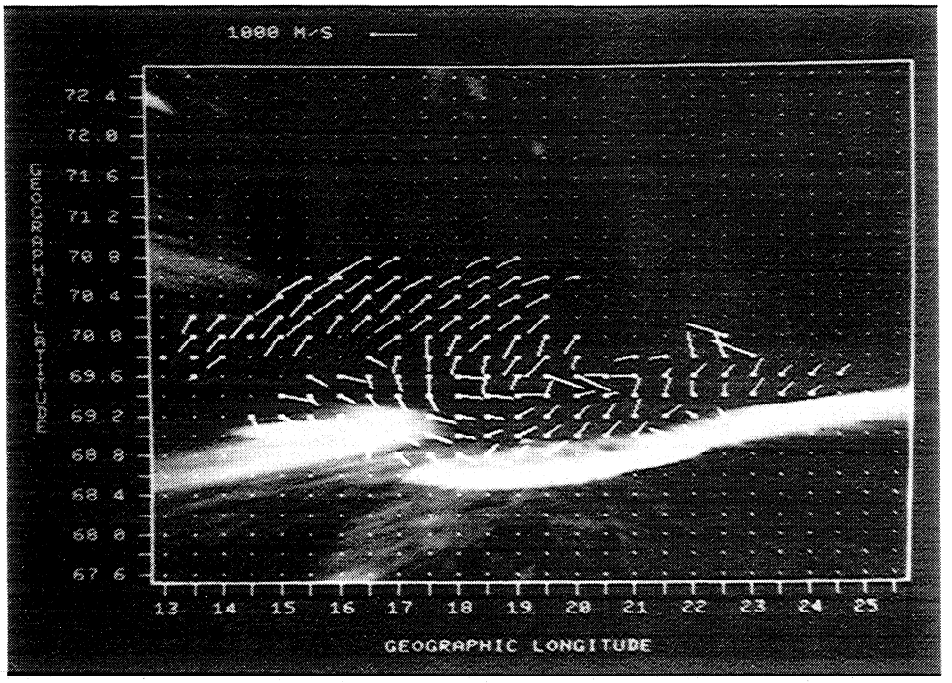

Figure 3. A mapping of Figure 2 onto a rectilinear geographic grid, at an altitude of 100 km, to remove the all-sky spatial distortion. The apparent radial streaking in the image near the edges is partially due to the vertical extent of the aurora.

reported during the Harang Discontinuity [*Nielsen and Greenwald*, 1979]. They also reported plasma vortices during the Harang Discontinuity, but they were of a larger-scale size of hundreds of kilometers. In one case, a large-scale vortex even appeared to pass over two arcs.

The appearance of the plasma vortex at the same time as the sudden brightening of the auroral arc, as well as the fact that the drifting plasma vortex coincided with a distortion of the arc moving at the same speed, is strong evidence that the plasma vortex is causally related to the activation of the arc. *Timofeev et al.* [1987] show several examples of the appearance or intensification of a radar aurora associated with the brightening of a postmidnight auroral arc, consistent with our observation.

For the subsequent analysis, it is important to determine if the event occurred before or after the Harang discontinuity. Unfortunately, the signature of the Harang discontinuity could not be found in the STARE data. The Scandinavian magnetometer array (SMA) is a two-dimensional array of 36 magnetometers, with a spacing of 100–150 km, operated in northern Scandinavia during the International Magnetospheric Study (IMS) [*Küppers et al.*, 1979]. Figure 4 shows SMA data from the closest station to Skibotn, at Rostadalen (68.97°N,

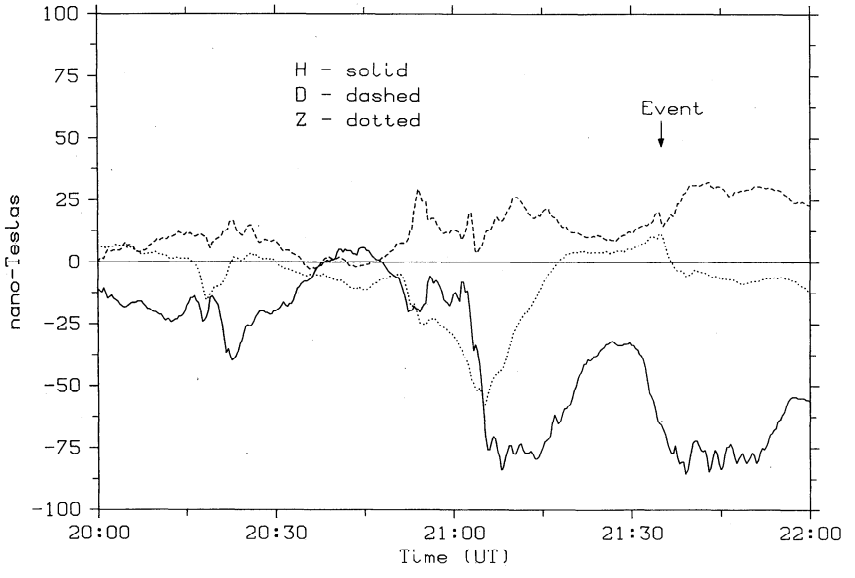

Figure 4. Ground-based Scandinavian magnetometer array (SMA) data, taken from Rostadalen (68.97°E, 19.67°N), showing the parallel H, perpendicular D, and vertical Z traces. The time of the event is indicated.

19.67°E), Norway. The magnetometer traces show moderately low activity. The time of the event is shown with negative H, indicating that it occurs during a small enhancement of the westward electrojet in the postmidnight convection region. Given the very quiet geomagnetic conditions prevailing, it is difficult to determine precisely the time at which the Harang discontinuity occurred. An examination of the magnetometer data from all northern SMA stations (not shown) indicates that the discontinuity passed over northern Scandinavia around 2000 UT or earlier. This is independently confirmed by magnetometer records (not shown) from Tromsø (69.66°N, 18.94°E) and Ny-Ålesund (78.92°N, 11.93°E).

The global statistical average electric field distribution for $Kp < 2$, in the geographic latitude range 63.4°–72.6° is shown in Figure 5, generated using a 180 day average of STARE and SABRE [*Nielsen et al.*, 1983] data combined, taken from 1982–1986. Arc segments indicate no radar backscatter. The latitude and time of the Harang discontinuity (HD) and the event (cross) are shown. The plot is orientated such that magnetic midnight is at the bottom. It is emphasized that the radar data are not from the time of the present event. Figure 5 shows the expected quiet time convection electric field which is poleward (equatorward) before (after) the discontinuity, statistically located around 2100 UT. For similar Kp, the Harang discontinuity may occur at different times on different days [*Nielsen and Greenwald*, 1979], hence Figure 5 is consistent with the discontinuity occurring around 2000 UT. Figure 5 reinforces the magnetometer observations that the Harang discontinuity occurred before the appearance of the plasma vortex under study. Note that the electric fields tend to be small, sometimes below the radar threshold, with ill-defined directions after the Harang discontinuity and around the event time. Normally,

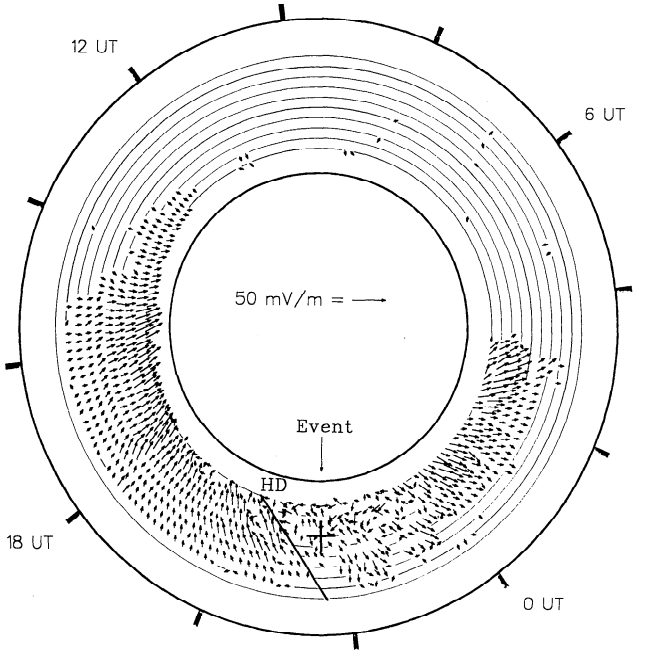

Figure 5. Globally statistical average electric field distribution from STARE and SABRE, for $Kp < 2$, in the geographic latitude range 63.4°–72.6°. Arc segments indicate no radar backscatter. The latitude and time of the Harang discontinuity (HD) and the event (cross) are shown. The radar data are a 180 day average taken from 1982 to 1986.

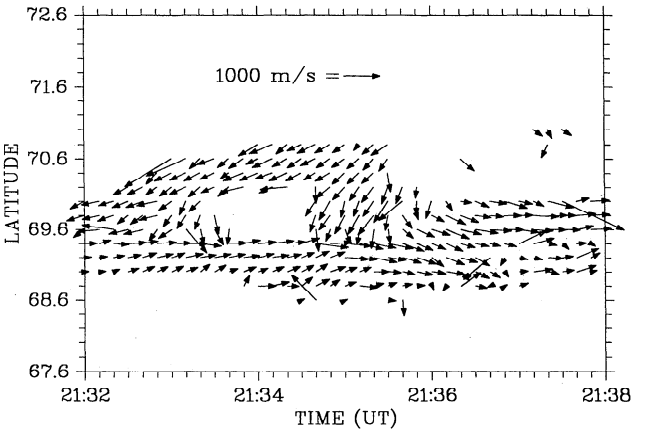

Figure 6. Temporal evolution of the plasma drift pattern. Latitudinal variation of the flow vectors obtained from 19.5°E is plotted against time. A region of anticlockwise turning vectors occurs between 2134 and 2136 UT.

STARE data are used only to estimate electric fields if the backscatter power exceeds 2 dB. In order to clearly observe the plasma vortex (see Figures 2 and 7) for the analysis, it was necessary to use a threshold of 1 dB, an indication of low ionospheric electric field strengths.

No radar backscatter was observed in the far poleward part of the STARE field of view or anywhere within or equatorward of the arc (see Figures 2 and 3), indicating small ionospheric electric fields of <15 mV/m [*Cahill et al.*, 1978]. Given the very quiet geomagnetic conditions prevailing ($Kp = 1^+$; see Figure 1) and that the convection electric field is frequently below the STARE detection threshold in the Harang discontinuity [*Nielsen and Greenwald*, 1979], this indicates that the observed plasma vortex is probably entirely due to mechanisms associated solely with the arc.

The temporal evolution of the plasma drift pattern is shown in Figure 6 in the form of a latitude-time diagram. The latitudinal variation of the drift velocity vectors, obtained from 19.5°E, is plotted with a time increment of 10 s. A region of anticlockwise turning of drift vectors is present between 2134 and 2136 UT. The plasma flow is predominantly westward at higher latitudes and eastward at lower latitudes. This plasma flow configuration is consistent with the expected statistically average flows shown in Figure 5 in the vicinity of the event (cross). Similar instances of such observations have been presented by *Horwitz et al.* [1978].

E region plasma flow drifts observed by coherent backscatter radar may be simply converted into equivalent ionospheric horizontal electric fields by rotating the vector clockwise through 90° and setting 1000 m/s = 50 mV/m ($V = E \times B$). Using this transform, Figure 7 shows the ionospheric horizontal electric field distribution at 2135 UT on January 15, 1980, in geographic coordinates. The lower border of the arc, projected at 100 km altitude, is also shown. The electric field vectors near the arc, corresponding to eastward plasma flow (see Figures 3 and 6), point approximately toward the arc. This result is not unexpected, as it indicates a horizontal ionospheric current flowing into the arc, which is necessary to feed the upward field-aligned current normally present in arcs [e.g., *Armstrong et al.*, 1975; *Kamide and Akasofu*, 1976a, b; *de la Beaujardiere et al.*, 1977; *Evans et al.*, 1977; *Cahill et al.*, 1980; *Robinson et al.*, 1981; *Marklund et al.*, 1982; *Brüning and Goertz*, 1986]. The

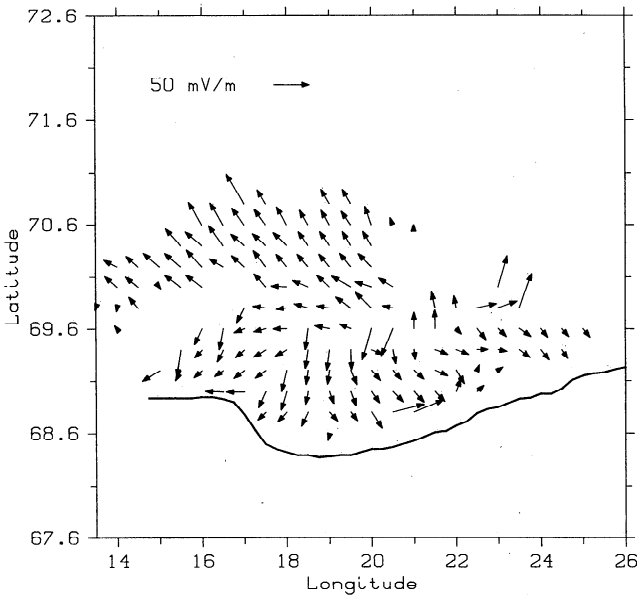

Figure 7. Ionospheric horizontal electric field distribution at 2135 UT on January 15, 1980, in geographic coordinates. The lower border of the arc, projected at 100 km altitude, is also shown.

electric fields north of the arc, corresponding to westward plasma flow, point approximately away from the arc. This suggests the possibility of a positive space charge in the region around 69.6°N, where the electric field reverses in order to account for the divergence of the electric field. *Aikio et al.* [1993] and *Timofeev et al.* [1987] have shown examples of the electric field enhancement adjacent to an auroral arc being simultaneous with the optical brightening of the arc. These are consistent with our observations.

3. Electrostatic Field Model

An early attempt was made to determine the electric field due to the arc just described using simple electrostatic field models based on the arc as a charged sheet [*Schoute-Vanneck*, 1988]. *Vondrak* [1975] proposed a scenario in which electrons flow along magnetic field lines into the arc (upward current), resulting in deposition of negative charge at altitudes where the electrons are stopped. The charge excess will eventually be neutralized by a return current from the magnetosphere into the ionosphere. This neutralization is presumably sufficiently slow that a negative charge temporarily builds up. Conductivity parallel to the magnetic field is ordinarily much larger than the perpendicular conductivity. Vondrak therefore expected that the return current would be equal in magnitude to and spatially coincident with the incident electron beam above the arc. Thus, in this picture, no net vertical (field aligned) currents would be detectable. To explain the existence of Birkeland field-aligned currents that are not spatially coincident with the arc, *Vondrak* [1975] postulates that net return charge flow is impeded in the region of the arc. This could occur if the acceleration of electrons is caused by a potential drop along magnetic field lines. This same potential drop will impede a return current above the arc, so that the return current must come from Birkeland currents in the region surrounding the arc. The negative space charge, within the arc, produces an electric field directed into the arc. Using a rocket, *Evans et al.* [1977] observed a boundary layer of negative space charge at the edge of an arc on the side where the ionospheric electric field was enhanced.

For initial modeling attempts, the arc, associated with the plasma vortex, was assumed to be a region of negative charge deposited by precipitating electrons. On a large spatial scale, if the arc is considered to be a horizontal line of point charges located only in the E region ionosphere, the variation of the electric field with distance from the arc r would be as $1/r^2$. An attempt to reproduce the observed electric field was made by integrating the effect of each charge element along the arc, taking the shape of the arc into consideration and adding a constant background convection electric field. The convection electric field was estimated from the STARE data farthest from the arc prior to the event. It was assumed that the background electric field was everywhere constant. This is a reasonable assumption since, for similar *Kp* levels, *Zi and Nielsen* [1980] found that the electric field varies by ~25% over the range of latitudes covered by the STARE field of view. The charge density of the arc and the threshold electric field of STARE could be varied at will in the model in order to achieve the best fit. However, with the $1/r^2$ assumption, no reasonable fit could be achieved. Modulating the charge density according to the brightness of the arc had little effect on the model.

By a change of spatial scale size, following a similar approach by *Opgenoorth et al.* [1983b], one may assume the arc to be made up of many field-aligned columns of negative charge along the length of the arc. The electric field due to each charge column decreases as $1/r$. The same procedure described above was employed. *Schoute-Vanneck* [1988] found that a rather good model reproduction of the observed electric field pattern could be made, provided that the fit was restricted to only poleward of the arc. Taking into account the lack of detectable radar backscatter equatorward of the arc, no reasonable fit could be achieved with the $1/r$ assumption. Further modeling attempts were made by including arbitrary regions of positive space without success. In most cases, the model's best fit occurred for the case of zero arc charge, i.e., no arc present.

It is an important feature that no radar backscatter is detected equatorward of the arc since an electrostatically charged arc should produce a quasi-symmetric electric field pattern in the vicinity of the arc. Including this fact makes it impossible to find any combination of a negatively charged arc, positively charged regions around the arc, and radar threshold that will reasonably reproduce the observed electric field in Figure 7. Hence it must be concluded that the arc and surrounding regions are free of excess charges. This is consistent with the findings of *Nielsen and Greenwald* [1979] for some arcs near the Harang Discontinuity. It is therefore concluded that the electric field pattern of Figure 7 must be the result of a combination of currents and conductivity. Given overall neutrality, it seems that polarization electric fields cannot exist in this event. The alternative suggestion of *Marklund* [1984], namely, that of Birkeland currents, was therefore pursued.

4. Birkeland Current Model

Given that the auroral arc results from electron precipitation, corresponding to a region of upward Birkeland current [e.g., *Kamide and Akasofu*, 1976a, b; *de la Beaujardiere et al.*, 1977], it is postulated here that the plasma vortex corresponds to the ionospheric signature of the closure current of the arc, thereby completing the circuit. *McDiarmid and McNamara*

[1978] and *Timofeev et al.* [1987] demonstrated that the region of radar backscatter contains downward field-aligned currents. The electric field pattern observed by STARE would be the result of field-aligned currents imposed by the magnetosphere combined with the Pedersen conductivity of the ionosphere [*Aikio et al.*, 1993].

The event occurred after the Harang Discontinuity and with a very low *Kp*. Convection electric fields may have values of only 20 mV/m during such geomagnetically quiet times [*Baumjohann*, 1983]. It has been shown that the discontinuity is generally associated with small convection electric fields (see Figure 5), and during these quiet geomagnetic conditions it is unlikely that the convection electric field makes any significant contribution. The fact that no radar backscatter is observed equatorward of the arc and in the far poleward part of the field of view indicates that any convection electric field present was probably <15 mV/m [*Cahill et al.*, 1978]. It seems entirely reasonable that the plasma vortex is a localized event purely associated with the auroral arc. In Figure 7 it is obvious that the plasma vortex corresponds to region of electric field divergence at ~69.6°N. For any given Pedersen conductivity this implies a region of horizontally divergent Pedersen current. Since current continuity must be preserved, the plasma vortex must correspond to a region of downward Birkeland current.

It is possible to make an estimate of the direction and strength of field-aligned currents by investigating the divergence of horizontal Pedersen currents [*Nielsen and Sofko*, 1982]. STARE provides the horizontal electric field distribution, but no estimate of the Pedersen conductivity is available. *Schlegel* [1988] has shown, from European Incoherent Scatter (EISCAT) radar data taken near Skibotn, that the height-integrated Pedersen conductivity is typically <4 S for low *Kp*. From a rocket shot through the Harang Discontinuity, *Behm et al.* [1979] found background height-integrated conductivities of 2 S or less. Since we have no information as to the variation of the Pedersen conductivity over the STARE field of view, we have simply assumed, for modeling purposes, a uniform value of 1 S everywhere.

The equivalent field-aligned current distribution is shown in Figure 8. Circles and crosses represent downward and upward currents, respectively. The lower border of the arc, projected at 100 km altitude, is also shown. In most of the field of view, the field-aligned current is small and predominantly downward, consistent with the observations of *McDiarmid and McNamara* [1978]. At about 69.6° latitude and between 19° and 24° longitude there is a region of strong downward current (0.8–2.8 $\mu A/m^2$), ~100 km poleward of and approximately parallel to the arc. The region is narrow, having an apparent latitudinal width of about 20 km, which is the spatial resolution of STARE. This is consistent with *Timofeev et al.* [1987], who found the meridional width of the downward current within the radar arc to be a few tens of kilometers. The zonal extent of strong downward current is ~160 km, less than half that of the arc.

Since the plasma vortex is causally linked to the arc, it must follow that the region of downward current is likewise causally linked to the arc, i.e., a region of upward current. Hence, for the first time from ground-based data, we have been able to identify the localized region, associated with an auroral arc, constituting a closed current sheet pair linked to the magnetosphere. Although the field-aligned current amplitudes appear quite reasonable [e.g., *Armstrong et al.*, 1975; *de la Beaujardiere et al.*, 1977; *Brüning and Goertz*, 1986; *Cahill et al.*, 1980; *Evans et al.*, 1977; *Marklund et al.*, 1982; *Robinson et al.*, 1981], it is stressed that these are estimates because we have no measurement of the Pedersen conductivity. However, the direction of the current is not affected.

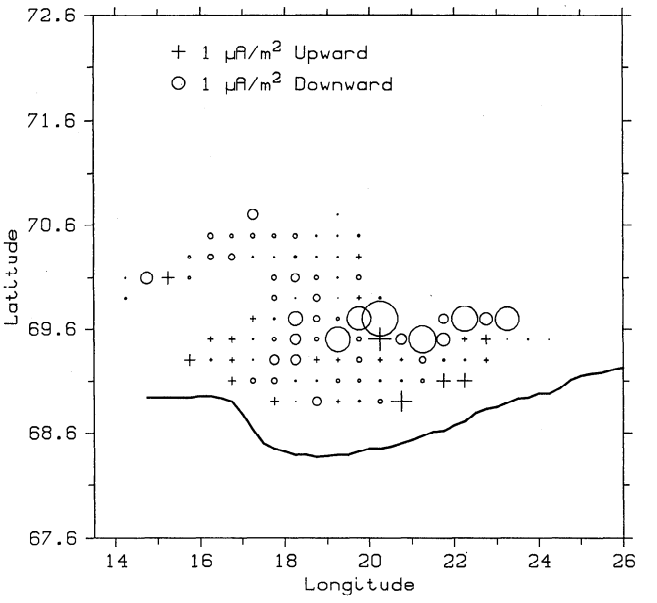

Figure 8. Equivalent field-aligned current distribution assuming a Pedersen conductivity of 1 S. Circles and crosses represent downward and upward currents, respectively. The lower border of the arc, projected at 100 km altitude, is also shown.

Tsunoda et al. [1976] and *Timofeev et al.* [1987] showed that the radar aurora corresponds to downward field-aligned currents, which are linked to the visual aurora by an ionospheric Pedersen current. It is well known that that an ionospheric electric field enhancement occurs poleward (equatorward) of an auroral arc when the large-scale background convection electric field points equatorward (poleward) [e.g., *Evans et al.*, 1977; *Horwitz et al.*, 1978; *Cahill et al.*, 1980; *Stiles et al.*, 1980; *de la Beaujardiere et al.*, 1981; *Marklund et al.*, 1982; *Ziesolleck et al.*, 1983; *Brüning and Goertz*, 1986; *Timofeev et al.*, 1987; *Opgenoorth et al.*, 1990; *Valladares and Carlson*, 1991; *Aikio et al.*, 1993; *Lewis et al.*, 1994], which is the case for after (before) the Harang Discontinuity. Such an enhancement is necessary to support the horizontal ionospheric Pedersen current required by the upward field-aligned current within an auroral arc [*Aikio et al.*, 1993]. The magnitude of the enhancement will depend on the ionospheric conductivity adjacent to the arc, which may be relatively low [*Aikio et al.*, 1993, and references therein]. This is indeed what we have observed.

Unfortunately, it is difficult to make a quantitative analysis of the field-aligned current, as we have no simple way to estimate the ionospheric Pedersen conductivity distribution or the particle flux corresponding to the auroral arc. Neither the EISCAT incoherent backscatter radar [*Folkestad et al.*, 1983] was available, nor were the TV images calibrated in intensity. The possibility of using the STARE electric field distribution combined with the SMA equivalent current field distribution is being investigated in order to obtain the height-integrated conductivity distribution [*Baumjohann et al.*, 1981; *Amm*, 1998] for this event. This would permit a quantitative estimate of the field-aligned currents. Using the 25 SMA stations still operating at the time of the event, it would also be possible to

reconstruct a three-dimensional equivalent current system associated with this event.

5. Black Aurora

East-west aligned black auroral filaments have been reported from Skibotn in the period 2139–2158 UT on January 15, 1980 [*Schoute-Vanneck et al.*, 1990]. A total of 186 examples were observed only 4 min after the event studied here from the same video data set. Several similarities are apparent between the region of downward field-aligned current (see Figure 8) and black auroras. The region of downward field-aligned current has a spatial dimension (200 × 20 km) that is much larger than that reported for black aurora (maximum 20 × 1.5 km). This implies that the region of downward current may correspond to a propagation channel, as described by *Schoute-Vanneck et al.* [1990], through which individual black aurora propagate. The drift speed of the plasma vortex (0.7–0.8 km/s) is within the range observed by *Trondsen and Cogger* [1997] for black auroras (0.6–1.5 km/s). Freja satellite observations have associated black aurora with low ionospheric conductivity (Pedersen conductance = 0.7 S) and downward field-aligned currents (2 $\mu A/m^2$) [*Marklund et al.*, 1994]. Using an assumed Pedersen conductance of 1 S, the plasma vortex observed by STARE is equivalent to a downward current of 0.8–2.8 $\mu A/m^2$ (see Figure 8). The same satellite data show strong diverging electric fields (up to 1 V/m) in small regions (<1 km) [*Marklund et al.*, 1995]. Taking into account the spatial resolution of STARE (20 × 20 km), this translates to an average electric field of up to 50 mV/m over one radar data cell. Such a diverging electric field is entirely consistent with our observations (see Figure 7).

Given the circumstantial evidence, it is natural to associate the observed return current region of the arc under study with black aurora. Unfortunately, no black auroras could be identified in the all-sky TV data owing to its relatively poor spatial resolution. Also, the return current region occurs about 28° off the magnetic zenith, which is close to the observable limit of 30° for black auroras [*Davis*, 1978]. The black auroras reported from Skibotn were observed using a low-light-level TV camera with a small field of view (23° × 30°) [*Schoute-Vanneck et al.*, 1990]. Unfortunately, the plasma vortex associated with the arc is not within this image [see *Schoute-Vanneck et al.*, 1990, Figure 5]. Nevertheless, it seems likely that the region of downward field-aligned current associated with the arc corresponds to a region of black auroras.

6. Conclusions

At a geomagnetically quiet time ($Kp = 1^+$) an auroral arc optically brightens following the passage of an eastward surge. This is causally related to a plasma vortex poleward of the arc in which plasma drift vectors rotate anticlockwise. It is shown that the event occurs after the Harang discontinuity and that it is consistent with previous similar observations. It has been demonstrated that the electric field pattern around the arc is not due to space charges but is consistent with a downward field-aligned current ~100 km poleward of the arc. The meridional width of this region is ~20 km or less, with a zonal extent of ~160 km, which is much less than the visual arc. The ground-based localization of the ionospheric signature of the magnetospheric current loop associated with the arc is a novel result.

Marklund [1984], who studied and classified arcs based on the electric field configuration around them, stated that polarization electric fields associated with auroral arcs tend to dominate when the background convection electric field is large. On the other hand, when the convection electric field is small, as is the case in this event, he found that Birkeland currents dominated the electric field pattern associated with the arc. The event studied here is entirely consistent with the latter.

Black auroras have been reported from Skibotn using the same video data set [*Schoute-Vanneck et al.*, 1990] only 4 min after the event studied here. The observed region of downward field-aligned current is entirely consistent with a region containing black auroras. Unfortunately, the video data are such that this cannot be conclusively determined. The combined use of STARE and a new digital all-sky imager (DASI) [*Kosch et al.*, 1998a] may provide a systematic approach to studying this poorly reported phenomenon.

It is possible that the ground-based identification of the closure current associated with the arc would not have been found were it not for the quiet geomagnetic conditions prevailing ($Kp = 1^+$) and the close proximity of the event to the Harang Discontinuity. Under active conditions or with the normal background convection electric field, the vortex signature may have been impossible to identify. Using STARE and DASI, it is planned to analyze other such events. It has been shown that the distribution of height-integrated Pedersen conductivity can be obtained by ground-based optical observations [*Kosch et al.*, 1998b] with an all-sky camera. This opens the future possibility for quantitatively estimating field-aligned currents.

Acknowledgments. Two of the authors (M.W.J.S.) and (M.J.K.) were each supported by a stipend from the Max-Planck-Gesellschaft. The STARE radars are operated by the Max-Planck-Institut für Aeronomie in cooperation with ELAB, the Norwegian Technical University (Trondheim), and the Finnish Meteorological Institute (Helsinki). The assistance of A. Korth and F. Both in processing the GEOS data as well as K.-H. Glassmeier and O. Amm in analyzing the SMA data is gratefully acknowledged.

The Editor thanks Hermann Opgenoorth and Göran Marklund for their assistance in evaluating this paper.

References

Aikio, A. T., H. J. Opgenoorth, M. A. L. Persson, and K. U. Kaila, Ground-based measurements of an arc-associated electric field, *J. Atmos. Terr. Phys.*, *55*, 797, 1993.

Amm, O., Method of characteritics in spherical geometry applied to a Harang discontinuity situation, *Ann. Geophys.*, *16*, 413, 1998.

Armstrong, J. C., S.-I. Akasofu, and G. Rostoker, A comparison of satellite observations of Birkeland currents with ground observations of visible aurora and ionospheric currents, *J. Geophys. Res.*, *80*, 575, 1975.

Balsley, B. B., W. L. Ecklund, and R. A. Greenwald, VHF Doppler spectra of radar echoes associated with a visual auroral form: Observations and implications, *J. Geophys. Res.*, *78*, 1681, 1973.

Baumjohann, W., Ionospheric and field-aligned current systems in the auroral zone: A concise review, *Adv. Space Res.*, *2*(10), 55, 1983.

Baumjohann, W., Electrodynamics of active auroral forms: Westward travelling surges and omega bands, in *Auroral Physics*, edited by C.-I. Meng, M. J. Rycroft, and L. A. Frank, p. 361, Cambridge Univ. Press, New York, 1991.

Baumjohann, W., R. J. Pellinen, H. J. Opgenoorth, and E. Nielsen, Joint two-dimensional observations of ground magnetic and ionospheric electric fields associated with auroral zone currents: Current systems associated with local auroral break-ups, *Planet. Space Sci.*, *29*, 431, 1981.

Behm, D. A., F. Primdahl, L. J. Zanetti Jr., R. L. Arnoldy, and L. J.

Cahill Jr., Ionospheric electrical currents in the late evening plasma flow reversal, *J. Geophys. Res.*, *84*, 5339, 1979.
Brüning, K., and C. K. Goertz, Dynamics of a discrete auroral arc, *J. Geophys. Res.*, *91*, 7057, 1986.
Cahill, L. J., R. A. Greenwald, and E. Nielsen, Auroral radar and rocket double probe observations of the lectric field across the Harang discontinuity, *Geophys. Res. Lett.*, *5*, 687, 1978.
Cahill, L. J., Jr., R. L. Arnoldy, and W. L. Taylor, Rocket observations at the northern edge of the eastward electrojet, *J. Geophys. Res.*, *85*, 3407, 1980.
Davis, T. N., Observed characteristics of auroral forms, *Space Sci. Rev.*, *22*, 77, 1978.
de la Beaujardiere, O., R. Vondrak, and M. Baron, Radar observations of electric fields and currents associated with auroral arcs, *J. Geophys. Res.*, *82*, 5051, 1977.
de la Beaujardiere, O., R. Vondrak, R. Heelis, W. Hanson, and R. Hoffman, Auroral arc electrodynamic parameters measured by AE-C and the Chatanika Radar, *J. Geophys. Res.*, *86*, 4671, 1981.
Evans, D. S., N. C. Maynard, J. Troim, T. Jacobsen, and A. Egeland, Auroral vector electric field and particle comparisons, 2, Electrodynamics of an arc, *J. Geophys. Res.*, *82*, 2235, 1977.
Fejer, B. J., and M. C. Kelley, Ionospheric irregularities, *Rev. Geophys.*, *18*, 401, 1980.
Folkestad, K., T. Hagfors, and S. Westerlund, EISCAT: An updated descripion of technical characteristics and operational capabilities, *Radio Sci.*, *18*, 867, 1983.
Greenwald, R. A., W. L. Ecklund, and B. B. Balsey, Auroral currents, irregularities, and luminosity, *J. Geophys. Res.*, *78*, 8193, 1973.
Greenwald, R. A., W. Weiss, E. Nielsen, and N. R. Thomson, STARE: A new radar auroral backscatter experiment in northern Scandinavia, *Radio Sci.*, *13*, 1021, 1978.
Hallinan, T. J., and T. N. Davis, Small-scale auroral arc distortions, *Planet. Space Sci.*, *18*, 1735, 1970.
Horwitz, J. L., J. R. Doupnik, and P. M. Banks, Chatanika radar observations of the latitudinal distributions of auroral zone electric fields, conductivities, and currents, *J. Geophys. Res.*, *83*, 1463, 1978.
Kamide, Y., and S.-I. Akasofu, The location of the field-aligned currents with respect to discrete arcs, *J. Geophys. Res.*, *81*, 3999, 1976a.
Kamide, Y., and S.-I. Akasofu, The auroral electrojet and field-aligned current, *Planet. Space Sci.*, *24*, 203, 1976b.
Korth, A., G. Kremser, and B. Wilken, Observations of substorm-associated particle flux variations at $6 < L < 8$ with GEOS-1, *Space Sci. Rev.*, *22*, 501, 1978.
Kosch, M. J., E. Nielsen, and T. Hagfors, A new Digital All-Sky Imager experiment for optical auroral studies in conjunction with the STARE coherent radar system, *Rev. Sci. Instrum.*, *69*, 578, 1998a.
Kosch, M. J., T. Hagfors, and K. Schlegel, Extrapolating EISCAT height-integrated Pedersen conductivities to other parts of the sky using ground-based auroral images, *Ann. Geophys.*, 16,583, 1998b.
Küppers, F., J. Untied, W. Baumjohann, K. Lange, and A. G. Jones, A two-dimensional magnetometer array for ground-based observations of auroral zone electric currents during the International Magnetospheric Study (IMS), *J. Geophys.*, *46*, 429, 1979.
Lewis, R. V., P. J. S. Williams, G. O. L. Jones, H. J. Opgenoorth, and M. A. L. Persson, The electrodynamics of a drifting arc, *Ann. Geophys.*, *12*, 478, 1994.
Marklund, G., Auroral arc classification scheme based on the observed arc-associated electric field pattern, *Planet. Space Sci.*, *32*, 193, 1984.
Marklund, G., I. Sandahl, and H. J. Opgenoorth, A study of the dynamics of a discrete auroral arc, *Planet. Space Sci.*, *30*, 179, 1982.
Marklund, G., L. Blomberg, C.-G. Fälthammer, and P.-A. Lindqvist, On intense diverging electric fields associated with black aurora, *Geophys. Res. Lett.*, *21*, 1859, 1994.
Marklund, G., L. Blomberg, C.-G. Fälthammer, P.-A. Lindqvist, and L. Eliasson, On the occurrence and characteristics of intense low-altitude electric fields observed by Freja, *Ann. Geophys.*, *13*, 704, 1995.
McDiarmid, D. R., and A. G. McNamara, Radio aurora in the dayside auroral oval spatial relationship with field-aligned currents and energetic particles, *J. Geophys. Res.*, *83*, 3226, 1978.
Mishin, E. V., and M. Förster, 'Alfvénic shocks' and low-altitude auroral acceleration, *Geophys. Res. Lett.*, *22*, 1745, 1995.
Nielsen, E., and A. Greenwald, Electron flow and visual aurora at the harang discontinuity, *J. Geophys. Res.*, *84*, 4189, 1979.
Nielsen, E., and G. Sofko, Ps 6 spatial and temporal structure from STARE and riometer observations, *J. Geophys. Res.*, *87*, 8157, 1982.
Nielsen, E., W. Güttler, E. C. Thomas, C. P. Stewart, T. B. Jones, and A. Hedberg, A new radar auroral backscatter experiment, *Nature*, *304*, 712, 1983.
Opgenoorth, H. J., and W. Baumjohann, Proceedings of conference achievements of the IMS, 26–28 June, Graz, Austria, *Eur. Space Agency Spec. Publ., ESA SP 217*, 365, 1984.
Opgenoorth, H. J., R. J. Pellinen, W. Baumjohann, E. Nielsen, G. Marklund, and L. Eliasson, Three-dimensional current flow and particle precipitation in a westward travelling surge (observed during the barium-GEOS rocket experiment), *J. Geophys. Res.*, *88*, 3138, 1983a.
Opgenoorth, H. J., J. Oksman, K. U. Kaila, E. Nielsen, and W. Baumjohann, Characteristics of eastward drifting omega bands in the morning sector of the auroral oval, *J. Geophys. Res.*, *88*, 9171, 1983b.
Opgenoorth, H. J., I. Häggström, P. J. S. Williams, and G. O. L. Jones, Regions of strongly enhanced perpendicular electric fields adjacent to auroral arcs, *J. Atmos. Terr. Phys.*, *52*, 449, 1990.
Parsons, N. R., and I. L. Thomas, Spatially forbidden regions in the aurora, *Can. J. Phys.*, *51*, 1377, 1973.
Robinson, R. M., E. A. Bering, R. R. Vondrak, H. R. Anderson, and P. A. Cloutier, Simultaneous rocket and radar measurements of currents in an auroral arc, *J. Geophys. Res.*, *86*, 7703, 1981.
Schlegel, K., Auroral zone E-region conductivities during solar minimum derived from EISCAT data, *Ann. Geophys.*, *6*, 192, 1988.
Schoute-Vanneck, H., Aurorae and plasma convection, Ph. D. thesis, Univ. of Natal, Durban, South Africa, 1988.
Schoute-Vanneck, H., M. W. J. Scourfield, and E. Nielsen, Drifting black aurorae?, *J. Geophys. Res.*, *95*, 241, 1990.
Shukla, P. K., G. T. Birk, and R. Bingham, Vortex streets driven by sheared flow and applications to black aurora, *Geophys. Res. Lett.*, *22*, 671, 1995.
Stiles, G. S., J. C. Foster, and J. R. Doupnik, Prolonged radar observations of an auroral arc, *J. Geophys. Res.*, *85*, 1223, 1980.
Timofeev, E. E., M. K. Vallinkoski, T. V. Jozelova, A. G. Yahnin, and R. J. Pellinen, Systematics of arc-associated electric fields and currents as inferred from radar backscatter measurements, *J. Geophys.*, *61*, 122, 1987.
Trondsen, T. S., and L. L. Cogger, High-resolution television observations of black aurora, *J. Geophys. Res.*, *102*, 363, 1997.
Tsunoda, R. T., R. I. Presnell, and T. A. Potemra, The spatial relationship between the evening radar aurora and field-aligned currents, *J. Geophys. Res.*, *81*, 3791, 1976.
Valladares, C. E., and H. C. Carlson Jr., The electrodynamics, thermal and energetic character of intense sun-aligned arcs in the polar cap, *J. Geophys. Res.*, *96*, 1379, 1991.
Vondrak, R. R., Model of Birkeland currents associated with an auroral arc, *J. Geophys. Res.*, *80*, 4011, 1975.
Zi, M., and E. Nielsen, Spatial variations of ionospheric electric fields at high latitudes on magnetic quiet days, in *Exploration of the Polar Upper Atmosphere*, edited by C. S. Deehr and J. A. Holtet, p. 293, D. Reidel, Norwell, Mass., 1980.
Ziesolleck, C. H., W. Baumjohann, K. Brüning, C. W. Carlsson, and R. I. Bush, Comparison of height-integrated current densities derived from ground-based magnetometer and rocket-borne observations during the Porcupine F3 and F4 flights, *J. Geophys. Res.*, *88*, 8063, 1983.

M. J. Kosch and E. Nielsen, Max-Planck-Institut für Aeronomie, Max-Planck-Strasse 2, 37191 Katlenburg-Lindau, Germany. (kosch@linax1.mpae.gwdg.de)
M. W. J. Scourfield, Space Physics Research Institute, University of Natal, 4001 Durban, South Africa.

(Received December 17, 1997; revised May 19, 1998; accepted July 17, 1998.)